Plasma Phys. Control. Fusion **51** (2009) 044001 (17pp) doi:10.1088/0741-3335/51/4/044001

Effect of gas injection during LH wave coupling at ITER-relevant plasma–wall distances in JET

A Ekedahl[1], K Rantamäki[2], M Goniche[1], J Mailloux[3], V Petrzilka[4], B Alper[3], Y Baranov[3], V Basiuk[1], P Beaumont[3], G Corrigan[3], L Delpech[1], K Erents[3], G Granucci[5], N Hawkes[3], J Hobirk[6], F Imbeaux[1], E Joffrin[1], K Kirov[6], T Loarer[1], D McDonald[3], M F F Nave[7], I Nunes[7], J Ongena[8], V Parail[3], F Piccolo[3], E Rachlew[9], C Silva[7], A Sirinelli[3], M Stamp[3], K-D Zastrow[3] and JET-EFDA contributors[10]

JET-EFDA, Culham Science Centre, OX14 3DB, Abingdon, UK
[1] CEA, IRFM, F-13108 Saint-Paul-lez-Durance, France
[2] Association Euratom-Tekes, VTT, PO Box 1000, FI-02044 VTT, Espoo, Finland
[3] Association Euratom-UKAEA, Culham Science Centre, Abingdon, Oxon, OX14 3DB, UK
[4] Association Euratom-IPP.CR, IPP AS CR, Za Slovankou 3, 182 21 Praha 8, Czech Republic
[5] Association Euratom-ENEA sulla Fusione, IFP Milano, Italy
[6] Association Euratom-MPI für Plasmaphysik D-85748 Garching, Germany
[7] Association Euratom-IST, Centro de Fusão Nuclear, IST, 1049-001 Lisbon, Portugal
[8] Association Euratom-Belgian State, ERM-KMS, B-1000 Brussels Belgium
[9] Association Euratom-VR, Department of Physics, SCI, KTH, SE-10691 Stockholm, Sweden

E-mail: annika.ekedahl@cea.fr

Received 17 July 2008, in final form 27 October 2008
Published 18 March 2009
Online at stacks.iop.org/PPCF/51/044001

Abstract

Good coupling of lower hybrid (LH) waves has been demonstrated in different H-mode scenarios in JET, at high triangularity ($\delta \sim 0.4$) and at large distance between the last closed flux surface and the LH launcher (up to 15 cm). Local gas injection of D_2 in the region magnetically connected to the LH launcher is used for increasing the local density in the scrape-off layer (SOL). Reciprocating Langmuir probe measurements magnetically connected to the LH launcher indicate that the electron density profile flattens in the far SOL during gas injection and LH power application. Some degradation in normalized H-mode confinement, as given by the H98(y,2)-factor, could be observed at high gas injection rates in these scenarios, but this was rather due to total gas injection and not specifically to the local gas puffing used for LH coupling. Furthermore, experiments carried out in L-mode plasmas in order to evaluate the effect on the LH current drive efficiency, when using local gas injection to improve the coupling, indicate only a small degradation ($\Delta I_{\mathrm{LH}}/I_{\mathrm{LH}} \sim 15\%$). This effect

[10] See annex of Watkins M *et al* 2006 *Proc. 21st Int. Conf. on Fusion Energy 2006 (Chengdu, China)* (Vienna: IAEA) OV/1-3.

is largely compensated by the improvement in coupling and thus increase in coupled power when using gas puffing.

(Some figures in this article are in colour only in the electronic version)

1. Introduction

Lower hybrid (LH) waves are one of the most efficient methods for non-inductive current drive (CD) generation in a tokamak. LH waves have the property of damping efficiently at high parallel phase velocities, $v_\parallel$, relative to the electron thermal speed [1]. They are therefore well suited for driving current off-axis in the plasma where the electron temperature is lower. Localized current off-axis gives a method for current profile control, which is crucial for the so-called advanced tokamak scenarios relying on the formation of an internal transport barrier (ITB) [2]. Lower hybrid current drive (LHCD) is used routinely in the advanced tokamak scenarios in JET, both for tailoring the target q-profile in the plasma current ramp-up phase before the main heating, as well as during the main heating phase in order to maintain the desired q-profile for longer duration [3].

The coupling of the slow wave to the plasma is a crucial issue, in particular for the next step device, ITER. The presence of a cut-off density, $n_{\rm co}$, below which the slow wave does not propagate, necessitates the ability to control the electron density in front of the LH launcher. The cut-off density corresponds to the density at which the launched wave frequency equals the local electron plasma frequency. This gives $n_{\rm co} = 0.0124 \times f^2$, where f is the launched wave frequency. For the LHCD system in JET, which operates at $f = 3.7\,\text{GHz}$, $n_{\rm co}$ equals $1.7 \times 10^{17}\,\text{m}^{-3}$. In the present day machines, the appropriate electron density for coupling conditions (typically 2–5 $\times$ $n_{\rm co}$) can be obtained by moving the launcher or the plasma radially during the pulse. However, in ITER, the launcher will be embedded in the first wall and the distance between the first wall and the last closed flux surface (LCFS) of the plasma will be as large as 15–20 cm. In addition, the H-mode with its edge transport barrier causes a steep gradient in electron density, which makes the electron density at the first wall drop during the period between ELMs. Consequently, it is essential to demonstrate the feasibility of coupling LH waves on present day devices, in conditions as close as possible to those of ITER, and thus to find suitable methods for controlling the electron density.

In JET, local gas injection in the vicinity of the LH launcher has proven efficient for raising the electron density in front of the launcher, thereby improving the LH coupling. The idea of a local gas injection system originates from the results obtained in ASDEX [4] and such a system is now used routinely when coupling LH waves in H-mode plasmas in JET. Because of its size, JET is a unique device which enables coupling studies over large plasma–launcher distances, close to those expected in ITER. In recent campaigns, dedicated LH coupling experiments have been performed in ELMy H-mode plasmas with high triangularity, with q-profiles characteristic of the advanced tokamak scenario ($q_{95} \sim 5.5$–7) as well as the hybrid scenario ($q_{95} \sim 4$). In addition to the effect on the LH coupling, these experiments allowed to investigate the effect of gas puffing on the confinement properties of the plasma, in order to assess possible deleterious effects when using gas puffing for LH coupling control. The question of a possible degradation in LH CD efficiency when using near gas injection was addressed in a recent experiment, carried out in L-mode plasmas.

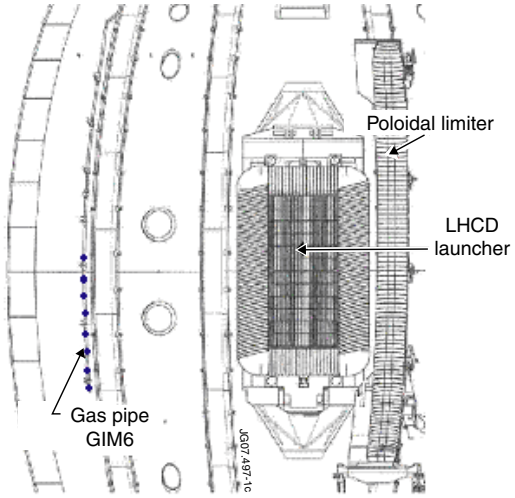

Figure 1. Front view of the LH launcher in JET. The gas injection pipe (GIM6) is seen to the left of the launcher and a poloidal limiter to the right. The eight points indicate the outlets from the pipe. To the right of the poloidal limiter is an ICRH antenna (not shown in the figure).

2. The LH launcher in JET

The LH launcher at JET [5, 6] operates at $f = 3.7$ Hz and is composed of 48 multijunctions, made of copper coated stainless steel and mounted in 6 rows and 8 columns. The 48 multijunctions are fed by 24 klystrons, each capable of delivering 500 kW for 20 s. At the front face of each multijunction there are two rows with four narrow waveguides, with dimensions 9 mm $\times$ 72 mm. The total size of the launcher is therefore 0.9 m height and 0.4 m width, consisting of twelve rows with 32 active waveguides. The $n_\parallel$-spectrum radiated from the launcher is usually centred at $n_\parallel = 1.84$ but can be varied between 1.4 and 2.3 by varying the phase difference between klystrons feeding adjacent multijunctions. $n_\parallel = 1.84$ and 2.3 was used in the experiments presented in this paper. The full width of both spectra is $\Delta n_\parallel = 0.45$.

The launcher mouth is surrounded by a side protection frame to protect it from plasma radiation. In addition, poloidal limiters are positioned around the outer wall of the torus, protruding in front of the LH launcher and the ion cyclotron resonance heating (ICRH) antennas. In order to allow for good coupling in different plasma conditions, the launcher can be moved radially during the pulse. Typically the launcher is positioned between 5 and 25 mm behind the poloidal limiters.

In addition to the launcher position control, good coupling is achieved using a dedicated gas injection pipe, denoted GIM6 (Gas Introduction Module 6), which provides local gas flow near the launcher. The pipe is located on the outer wall about 1.2 m from the launcher (figure 1). The first experiments with local gas injection for LH coupling were carried out in L-mode plasmas in 1996–1997 and later in H-mode plasmas from 2001 onwards, where both CD_4 injection [7] and D_2 injection [8] were used. D_2 injection proved to be more efficient than CD_4 to increase the electron density in the scrape-off layer (SOL), probably because D_2 gives higher recycling [8]. The previous LH coupling experiments in H-mode plasmas were limited mainly to low triangularity plasmas and to a distance between the LCFS and the LH launcher of 11 cm. In the work presented in this paper, good LH coupling was demonstrated in

H-mode plasmas at high triangularity, with maximum values of upper and lower triangularity of $\delta_{up} = 0.45$ and $\delta_{low} = 0.52$, and at LCFS–launcher distances up to 15 cm.

3. LH coupling in H-mode plasmas

3.1. Advanced tokamak scenario

In recent campaigns dedicated experiments were performed to demonstrate LH coupling at large plasma–launcher distances [9]. These experiments were performed in an ELMy H-mode scenario that was used for the development of advanced tokamak scenarios with ITB. However, since the experiments were performed early in the campaign during the development of the scenario, no ITBs were yet obtained. The magnetic field was between $B_T = 3.0$ T and 3.1 T and the plasma current was $I_p = 1.5$–1.9 MA, resulting in $q_{95} \sim 5.5$–7. In order to obtain an H-mode, neutral beam injection (NBI) power ranging from 14 to 18 MW was used. In addition, up to 3 MW ICRH power was used in some pulses. The LHCD power varied from 0 to 3.1 MW and the launcher position was 2 cm behind the poloidal limiter, while the LCFS was pushed 13 cm away from the poloidal limiters. This distance is also denoted radial outer gap (ROG). Figures 2 and 3 show two similar discharges in terms of injected powers, plasma position and GIM6 flow. The only difference between the two discharges is the fact that pulse #67882 has strong additional gas puffing from the gas injection points near the divertor region. One can note that the H_α signal is therefore higher, indicating higher recycling in #67882. As a consequence, the LH coupling during the period 4–6 s is better in #67882 (figure 2) than in #67884 (figure 3). In #67884, the ragged LHCD power waveform during the period 4–6 s is due to frequent interruptions caused by a launcher protection system that reduces the klystron output power when the reflected power is too high. When gas injection from GIM6 (4×10^{21} el s^{-1}) is switched on, the electron density increases, the reflection coefficient decreases and the coupled LHCD power is maintained above 2 MW. In addition, one can note that the ICRH power suffers fewer trips when GIM6 is switched on, showing that coupling of ICRH can also be improved by local gas puffing [10].

With gas injection from the divertor at a rate 20×10^{21} el s^{-1}, and without gas injection from GIM6, good LH coupling was obtained on the upper and middle part of the launcher, as is demonstrated in #67882, 4–6 s. Consequently, 2.4 MW was stationary coupled to the plasma for 5 s over a LCFS–launcher distance of 15 cm and a reflection coefficient as low as RC = 6%. However, the lower part of the launcher has a reflection coefficient of about $RC_{low} = 10\%$. This poor coupling could be linked to the fact that the lowest row is farthest away from the plasma. The distance between the LCFS and the poloidal limiter is 14 cm for the lowest row and 12–13 cm for the other rows. When gas is injected from GIM6, the coupling on the bottom row is improved and the reflection coefficient of that row is restored to $RC_{low} = 2\%$.

A reciprocating Langmuir probe (RCP) [11] was used to measure the far SOL plasma in between ELMs. This probe is located at the top of the torus. The plasma scenario was chosen in such a way that the probe was magnetically connected to the LH launcher and the gas pipe GIM6. The measurements were performed at $t = 5$ s and $t = 7$ s in #67884. Each reciprocation take approximately 200 ms. In order to avoid disturbing the probe signal due to ICRH, the ICRH power was decreased during the reciprocations. The radial profiles of the ion saturation current, J_{sat}, measured at two different times in #67884, are shown in figure 4. The ion saturation current can be considered proportional to the electron density. With gas puffing from GIM6 together with 2 MW of coupled LHCD power, the J_{sat}-profile flattens in the far SOL, i.e. typically between 8 and 15 cm from the LCFS (squares). At 15 cm, which is the radial location of the LH launcher, the ion saturation current is more than twice as large as

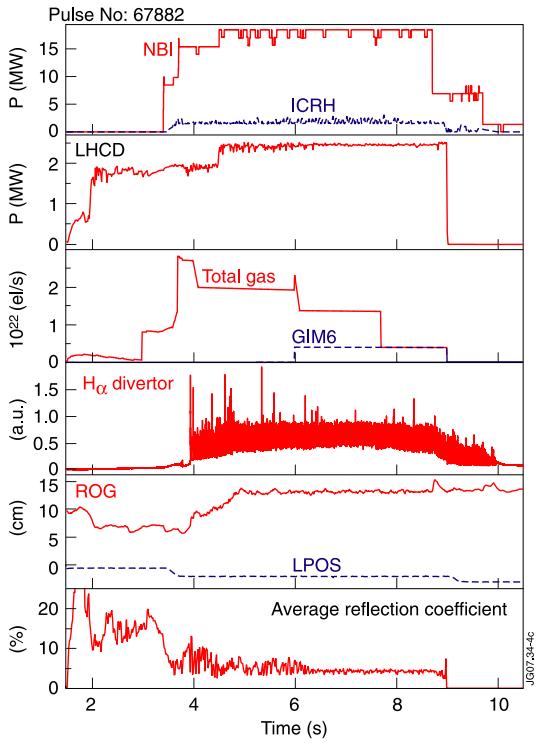

Figure 2. Illustration of long distance LH coupling, in a case with large gas flow from the divertor. Good coupling is obtained even without GIM6 injection (4–6 s). Shown as a function of time are NBI and ICRH powers, coupled LHCD power, total gas flow and near gas flow from GIM6, the H_α signal showing the ELM activity, the positions of the LCFS relative to the poloidal limiter (ROG) and the LH launcher relative to the poloidal limiter (LPOS), and the average reflection coefficient on the LH launcher.

compared with the case without gas injection (circles). The location of the poloidal limiter is indicated by the dashed line at 13 cm. However, closer to the separatrix, basically no difference is seen in J_{sat}.

3.2. Hybrid scenario at 1.7 T

For the first time in JET, LHCD power has been coupled during the H-mode phase of low toroidal magnetic field plasmas ($B_T = 1.7$ T, $I_P = 1.4$ MA, $q_{95} = 4$). This configuration was used for studying the hybrid scenario in JET [12] and its comparison with the standard H-mode scenario. The aim of the experiment was to demonstrate the LH coupling capability in high triangularity plasmas with large LCFS–launcher distance and during ELMs, in a similar way as in the advanced tokamak configuration described above. Also in this scenario at low toroidal magnetic field, good coupling of the LH wave was obtained at a distance between the LCFS and the launcher of 14 cm, using D_2 injection from GIM6. This is shown in figure 5, in which 2.7 MW of LHCD power is coupled during 8 s in an H-mode plasma with high frequency (>100 Hz), small amplitude ELMs. The gas flow near the launcher was 5×10^{21} el s^{-1} and the average power reflection coefficient was 4–6%.

From the LHCD point of view, the parameter to take into account in this low toroidal magnetic field scenario is the reduced accessibility of the LH wave. The accessibility condition,

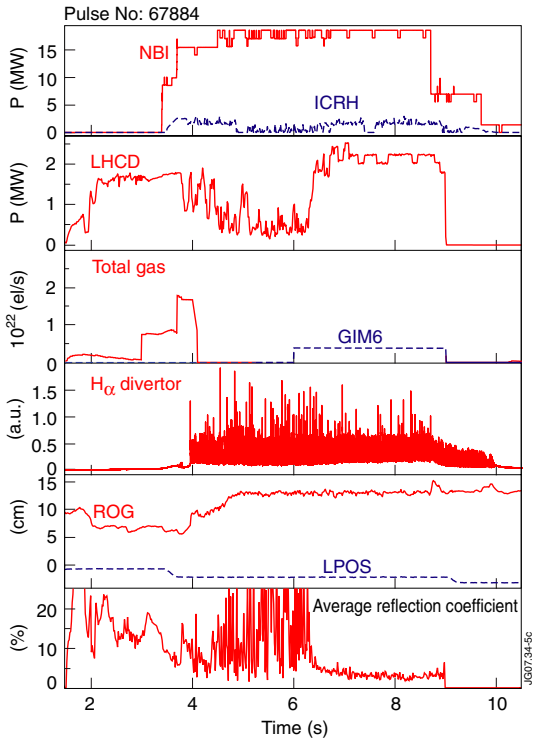

Figure 3. Illustration of the long distance LH coupling experiment, in a case with only GIM6 injection, or no gas injection, during the H-mode phase. The coupling is degraded over the whole launcher when no gas is injected (4–6 s).

$n_\parallel^{\rm acc}$, is given by [13, 14]

$$n_\parallel^{\rm acc} = \frac{\omega_{\rm pe}}{\omega_{\rm ce}} + \sqrt{1 + \left(\frac{\omega_{\rm pe}}{\omega_{\rm ce}}\right)^2 - \left(\frac{\omega_{\rm pi}}{\omega}\right)^2},$$

where ω is the wave frequency, $\omega_{\rm pe}$ the local electron plasma frequency, $\omega_{\rm pi}$ the local ion plasma frequency and $\omega_{\rm ce}$ the local electron cyclotron frequency, respectively. The LH wave accessibility therefore depends on the local electron density and magnetic field. Waves with $n_\parallel > n_\parallel^{\rm acc}$ are accessible to the plasma interior, while waves with $n_\parallel < n_\parallel^{\rm acc}$ will be reflected at that layer. For the scenario shown in figure 5, the minimum $n_\parallel$ accessible is as high as $n_\parallel^{\rm acc} \sim 3.0$ at $R = 3.7$ m ($r/a = 0.8$). Therefore, the highest $n_\parallel$-spectrum was also used in the experiment ($n_\parallel = 2.3$) and compared with the standard $n_\parallel$-spectrum peaked at 1.84, which corresponds to the highest power directivity. In plasmas suffering from poor LH wave accessibility, one may find increased impurity production, as reported in JT-60U [15]. However, in this JET experiment no difference in impurity production between $n_\parallel = 1.84$ and $n_\parallel = 2.3$ could be observed. The difference in coupling between the two phasings was small, although $n_\parallel = 1.84$ had a slightly lower reflection coefficient than $n_\parallel = 2.3$. A comparison of two consecutive discharges with different $n_\parallel$ spectra show that the average RC during the L-mode phase (4.0–4.5 s) was 4% for $n_\parallel = 1.84$, increasing to 6% for $n_\parallel = 2.3$. During the H-mode phase (5.5–7.0 s), the average RC was 7% for $n_\parallel = 1.84$, increasing to 8% for $n_\parallel = 2.3$. This is in agreement with SWAN code calculations, which predict a minimum in reflection coefficient for 0° phasing between adjacent multijunctions [16]. The 0° phasing ($n_\parallel = 1.84$)

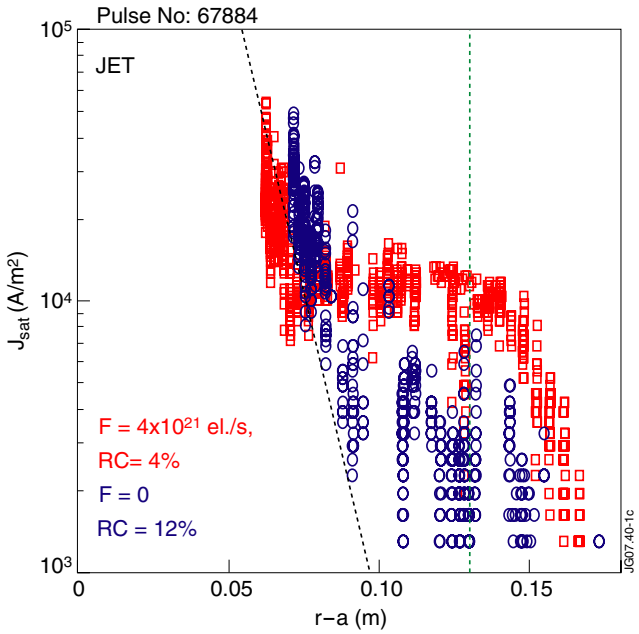

Figure 4. Ion saturation current measured by the reciprocating probe in #67884 as a function of the distance from the separatrix mapped to the mid-plane. With GIM6 and $P_{LH} = 2$ MW, $t = 7$ s (squares), without GIM6, $t = 5$ s (circles).

gives a continuous phase difference between the narrow waveguides at the grill mouth of 90°, which corresponds to the optimum feeding of the launcher and the highest power directivity.

4. Effects of gas puffing on plasma performance and LHCD efficiency

4.1. Effect on plasma performance

When using high levels of gas injection, a degradation in the H-mode confinement may be encountered due to reduced pedestal electron temperature and increased collisionality [17]. The series of discharges in the hybrid scenario experiment allowed to study the evolution of the normalized plasma pressure, β_N, and the normalized H-mode confinement, H98(y,2) [18]. In this experiment, β_N was controlled in real-time by adjusting the NBI power so as to maintain $\beta_N = 2.0$ between 6 and 7.5 s, and then $\beta_N = 2.5$ between 8 and 12 s. A typical NBI power waveform is shown in figure 5. Since the main aim was to reach large distance LH coupling conditions, the distance of the LCFS to the poloidal limiter and the GIM6 flow were increased from discharge to discharge. The LCFS–limiter distance (ROG) was varied between 4 and 12 cm, while the GIM6 flow was varied between 2×10^{21} and 8×10^{21} el s^{-1}. Figure 6 shows the values of ROG, GIM6 flow and LHCD power that were programmed for every discharge in the scan, averaged over the interval 6.0–7.5 s. As can be seen in the lower box of figure 6, an increase in the base-line level of the H_α-signal, viewing the divertor, was observed from discharge to discharge. This increase can be attributed to the increasing level of gas puffing. However, it is interesting to note that the discharges with $n_\parallel = 2.3$, as well as the discharge without LH during the main heating phase, give a lower value of H_α. Even though all the other parameters, such as gas injection, LCFS–limiter distance and LHCD power were the

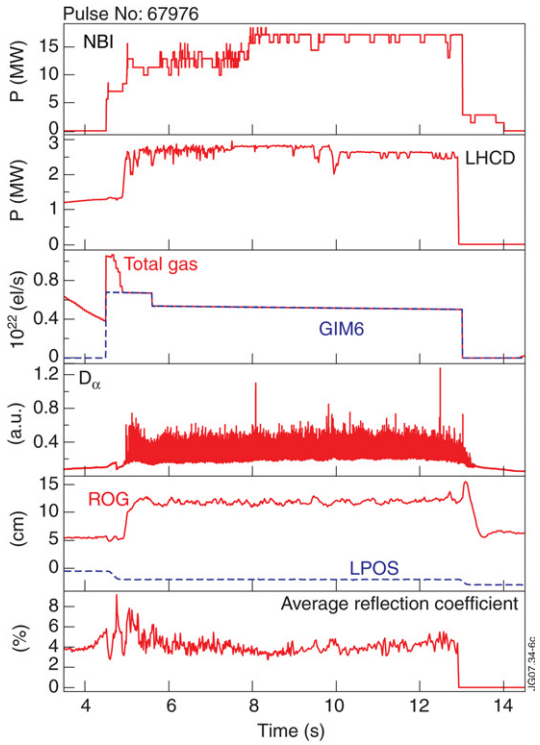

Figure 5. Illustration of LH coupling in hybrid scenario at $B_T = 1.7$ T. Shown are as a function of time: NBI and ICRH powers, coupled LHCD power, total gas flow and the near gas flow from GIM6, the H_α signal showing the ELM activity, the positions of the LCFS relative to the poloidal limiter (ROG) and the LH launcher relative to the poloidal limiter (LPOS) and the average reflection coefficient on the LH launcher.

same, the difference in H_α is noticeable. This difference may be attributed to the details of the LH wave propagation, either due to different LH wave accessibilities at the plasma periphery or to different LH power deposition profiles, as will be discussed later.

During this experiment, β_N was real-time controlled, with the NBI power as the actuator, in order to follow a pre-programmed waveform. In order to maintain the requested value of β_N, the NBI power had to increase from discharge to discharge. In fact, the increase in applied NBI power could therefore indicate a degradation in confinement due to the increased level of gas puffing. Figure 7 shows H98(y,2) at two different times, plotted versus the average electron density normalized to the Greenwald density limit, n_e/n_G [19]. As seen in figure 7, and as already observed in figure 6, the discharges with $n_\parallel = 2.3$, as well as the discharge without LH during the main heating phase, differ slightly from the rest of the data points. When instead H98(y,2) is plotted versus the base-line level of the divertor H_α-signal, a better correlation than with n_e/n_G is observed (figure 8). The figure suggests that higher recycling (higher H_α) can result in lower confinement. This finding is consistent with previous observations [20], as well as modelling efforts undertaken [21].

When using different $n_\parallel$ spectra of the injected LH wave, several differences can be expected. Firstly, it has to be noted that the internal inductance, especially during the LH pre-heat phase, was lower with $n_\parallel = 1.84$ than with $n_\parallel = 2.3$ ($\sim$0.80 compared with $\sim$0.85). The most probable reason for this is that the LH CD efficiency during the pre-heat phase is

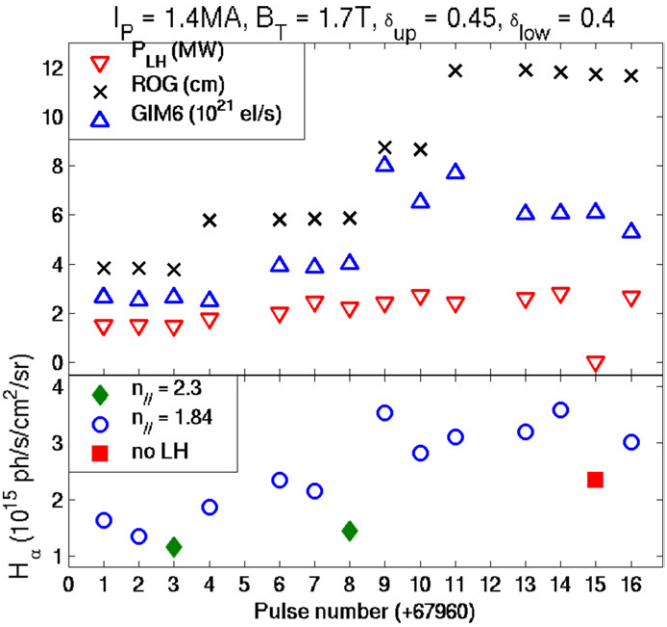

Figure 6. LHCD power, LCFS–limiter distance and GIM6 flow during the series of experiment in the Hybrid scenario configuration, in the time interval 6.0–7.5 s. The lower box shows the resulting base-line level of H_α-signal. Lower H_α is obtained for $n_\parallel = 2.3$ and without LHCD during the H-mode phase.

higher at lower $n_\parallel$, resulting in larger non-inductive current fraction. This is also supported by the fact that the loop voltage drop was larger for $n_\parallel = 1.84$ than for $n_\parallel = 2.3$ during the pre-heat phase. However, no difference in loop voltage could be seen during the main heating phase. In these discharges, the loop voltage was ∼100 mV during the high power phase with 15 MW NBI + 2–3 MW LHCD. Calculations with the DELPHINE code [22] coupled with CRONOS [23], for the parameters of pulse #67976 (figure 5), indicate that the non-inductive current fraction produced by LHCD was only approximately 10% of the total plasma current.

Secondly, different MHD activities were observed during the high performance phase. The MHD analysis made for pulse #67962, with $n_\parallel = 1.84$, indicates that a continuous $m = 3, n = 2$ mode remained throughout the high performance phase, while no MHD events associated with the so-called sawtooth or fishbone activities were observed. This indicates the absence of the $q = 1$ surface in the plasma. The lower H-mode confinement may therefore possibly be explained by the presence of the $m/n = 3/2$ mode, causing a degradation in confinement [24]. In contrast, in pulse #67963, with $n_\parallel = 2.3$, MHD activity associated with sawteeth and fishbones was detected, suggesting the presence of a $q = 1$ surface. The different current profiles in these two discharges were probably mainly due to the different pre-heat phases. When comparing the discharges with and without LHCD during the main heating phase, one observes a small decrease in internal inductance in the cases with LHCD (#67974 and #67976), compared with the reference case without LHCD (#67975). In addition, the sawtooth activity re-appears earlier in #67975 than in #67974 and #67976, which suggests that some difference in current profile does exist. However, no difference in loop voltage can be seen but, as mentioned above, the LH driven non-inductive current fraction is only ∼10%

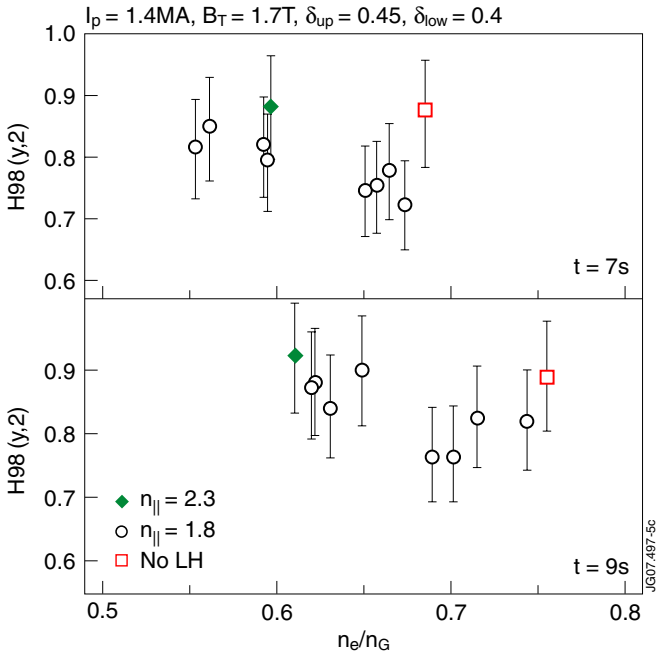

Figure 7. H98(y),2 versus n_e/n_G for the discharges in the hybrid scenario experiment at $B_T = 1.7$ T (figure 4). The pulse indicated as 'no LH' has only LHCD power in the pre-heat phase up to 5 s (with $n_{||} = 1.84$).

of the total plasma current in this low magnetic field scenario. It has to be noted that this experiment was a dedicated LH coupling experiment, and therefore not necessarily optimized to obtain the highest LH CD efficiency.

Thirdly, the LH wave accessibility is reduced for $n_{||} = 1.84$ during the high performance phase at high density. One could argue that this could lead to enhanced interaction with the plasma edge and increased recycling. However, it is not possible to conclude which factor is responsible for the lower H_α emission observed for $n_{||} = 2.3$ and without LHCD.

The results in figures 7 and 8 indicate a degradation in performance at increasing H_α level, mainly due to gas puffing from GIM6. However, these results do not allow one to distinguish between the effect of gas puffing from GIM6 (outer mid-plane) or from other gas flow locations (e.g. from the divertor). The experiment described in section 3.1 allows one to address this issue, since different combinations of gas injection locations were used. The scenario was the advanced tokamak scenario, but since the experiment was performed early during the development campaign, ITBs were not obtained. The H-mode was characterized by type I ELMs, for which the ELM frequency increased with increasing amount of gas puffing. Figure 9 shows H98(y,2) versus the electron density normalized to the Greenwald density limit, n_e/n_G, for discharges characterized by an upper triangularity $\delta_{up} = 0.38$–0.41 and $q_{95} = 5.5$–6.8. The various GIM6 levels can be distinguished. The data points corresponding to zero flow from GIM6 have gas injection from the divertor region at a level of $\sim 20 \times 10^{21}$ el s^{-1}. From figure 9, there does not seem to be any difference in confinement, whether GIM6 is used or not. However, further experiments are necessary in order to verify the experimental result of figure 9 in higher confinement scenarios, with H98(y,2) = 1 or above.

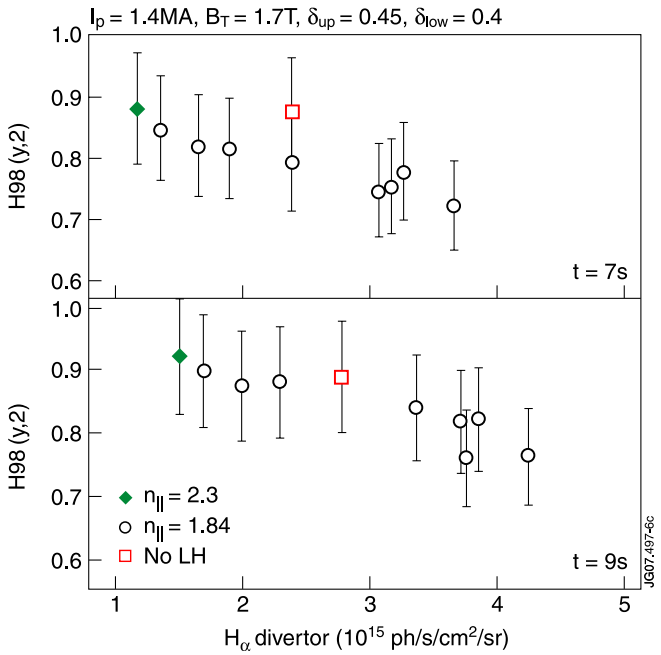

Figure 8. H98(y,2) versus the base-line level of the divertor H_α-signal, for the same discharges and time slices as in figure 7.

4.2. Effect on LH CD efficiency

When using near gas puffing to improve the LH coupling, possible deleterious effects due to parasitic absorption of the LHCD power in front of the launcher at excessive local electron density could be an important issue. Such effects could translate into increased heat flux carried by the electrons accelerated near the grill mouth and possibly a decrease in the LH CD efficiency. The figure of merit for the LH CD efficiency (η) is given by $\eta = RI_{\rm LH}n_{\rm e}/P_{\rm LH}$ (in units of 10^{20} Am^{-2} W^{-1}), where R is the plasma major radius, $n_{\rm e}$ the line average electron density, $I_{\rm LH}$ the LH driven non-inductive current and $P_{\rm LH}$ the LHCD power. An experiment has recently been carried out in JET in order to investigate this issue. For simplicity, it was carried out in L-mode plasmas with 2.8 MW LHCD, with the addition of 1 MW ICRH power in order to increase the plasma electron temperature thereby improving the LHCD efficiency. Real-time control on the boundary flux was used, in order to keep the loop voltage constant and leave the plasma current floating. The amount of gas injected near the LH launcher (from GIM6) and the distance from the LCFS to the poloidal limiter (ROG) were varied from discharge to discharge, while parameters such as electron density, electron temperature, total gas injection and LHCD power were kept the same. In such a way, a variation in the LH CD efficiency was detected by a variation in the resulting plasma current.

The plasma parameters for the two extreme cases in the scan are shown in figure 10. #69581 was characterized by short LCFS–limiter distance (4 cm) and no gas injection from GIM6, while #69582 had large LCFS–limiter distance (10 cm) and a gas flow of 4×10^{21} el s^{-1} from GIM6. The electron temperature profiles for the two pulses were very similar, with a central electron temperature of $T_{\rm e0} \sim 3$ keV. The highest plasma current was indeed obtained for the case with small LCFS–limiter distance without gas injection near the launcher (#69581), while the lowest plasma current was obtained in the other extreme case with 10 cm distance between

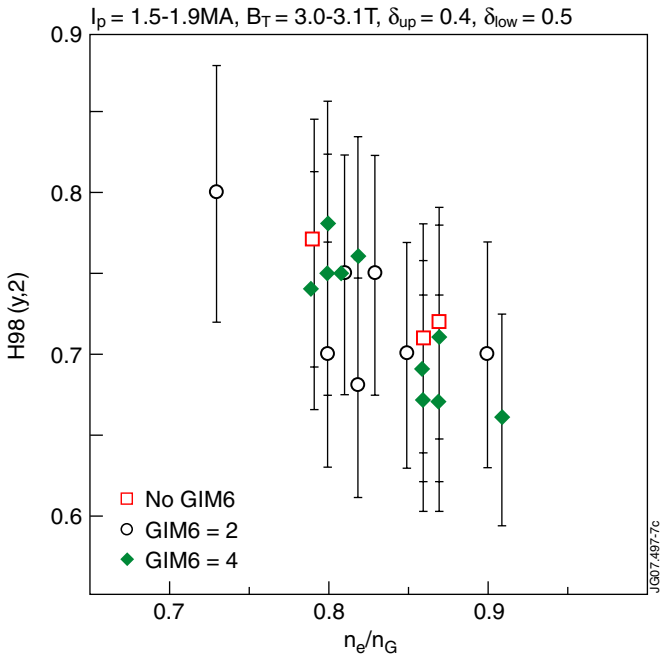

Figure 9. H98(y,2) versus n_e/n_G for high triangularity plasmas and advanced tokamak configuration (figures 2 and 3). The data is averaged over a 1s time period. GIM6 denotes the gas level from GIM6 in units of 10^{21} el s^{-1}.

the LCFS and the poloidal limiter and GIM6 injection (#69582). The value of Z_{eff}, as obtained from measurements along a horizontal chord, was higher in #69581 than in #69582 ($\sim$3.0 compared with $\sim$2.5). This is probably due to the proximity to the poloidal limiter in #69581. The Z_{eff}, obtained from measurements along a vertical chord, was identical up to 8.5 s ($\sim$2.0).

A higher amplitude and larger fluctuation level is seen on the divertor H_α-signal from 8 s onwards in #69582. Figure 11 shows the fluctuation level at the plasma periphery, slightly inside the LCFS, as measured by the O-mode reflectometry channel having its cut-off density at 1.1×10^{19} m^3. One can note that the lowest fluctuation level is clearly obtained for #69581, i.e. the discharge with small LCFS–limiter distance without GIM6, while the highest fluctuation levels are obtained for #69582 and #69576, which are the two discharges with the largest LCFS–limiter distance (10 cm) and gas injection from GIM6 with 4×10^{21} el s^{-1} and 2×10^{21} el s^{-1}, respectively. This result is possibly a first indication that LH wave scattering in the SOL region is enhanced in cases with a wide SOL combined with local gas puffing. LH wave scattering may modify the LH wave propagation, as described in [25].

Simulations with the DELPHINE code [22] coupled with CRONOS [23] for the parameters of #69581 indicate that the LH driven current was only 0.4 MA, i.e. approximately 30% of the total current. The bootstrap current was 0.1 MA. However, the density could not be maintained constant during the pulse (due to the gas puffing), which caused the current profiles (ohmic as well as LH driven current profile) to evolve during the pulse. Since stationary conditions were obtained in this experiment, it is difficult to accurately quantify the degradation in CD efficiency, as caused by large ROG and gas puffing. The simplest estimates would give the following: the difference in plasma current between the two extreme discharges, #69581 and #69582, is roughly 60 kA, which can be considered as the difference in LH driven current, i.e.

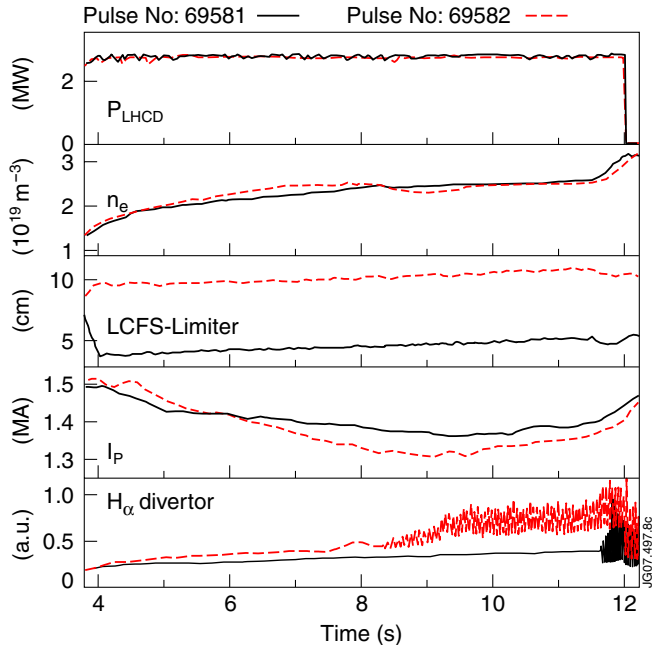

Figure 10. Evolution of plasma parameters for two discharges with real-time control on plasma boundary flux. Shown are: coupled LHCD power, line average electron density, LCFS–limiter distance (ROG), plasma current and divertor H_α-signal. #69581 has gas injection from the divertor, while #69582 has gas injection near the LH launcher.

$\Delta I_{\mathrm{LH}} \sim 60$ kA. CRONOS code modelling gives an absolute value of the LH driven current of $I_{\mathrm{LH}} \sim 400$ kA in this specific scenario. The drop in CD efficiency would therefore correspond to $\Delta I_{\mathrm{LH}}/I_{\mathrm{LH}} \sim 15\%$. Absorption of the LH waves by fast ions produced by ICRH, as reported in [26], was not likely occurring in this scenario, since the ICRH power used was only 1 MW. In addition, a similar estimate of the reduction in LH CD efficiency ($\Delta I_{\mathrm{LH}}/I_{\mathrm{LH}} \sim 15\% \pm 15\%$) was obtained in an earlier experiment in JET, carried out with LHCD alone [27]. Such a drop in LH CD efficiency is indeed small in comparison with the effect of the loss of coupled power that would be the result if local gas puffing was not used for improving the LH coupling at large distance. As an example, one can see in figure 3 that the coupled power drops by approximately 75% when GIM6 is not used. This will consequently result in 75% less non-inductively driven current by LHCD.

5. Modelling of gas puff

The density increase in front of the launcher has been studied numerically with the two-dimensional code EDGE-2D [28, 29]. For this purpose, the code has been extended to account for a SOL width of up to 10 cm. In this model, the effect of LHCD power is taken into account by assuming that a certain fraction of the power is absorbed within the narrow band in front of the launcher. Consequently, the plasma in this narrow band heats up locally and this then contributes to the ionization of the gas. This way the code takes into account the direct effect of LHCD power on the ionization. The poloidal limiters have been modelled as spatially localized sinks, where the recombination is artificially enhanced [30]. This makes it possible

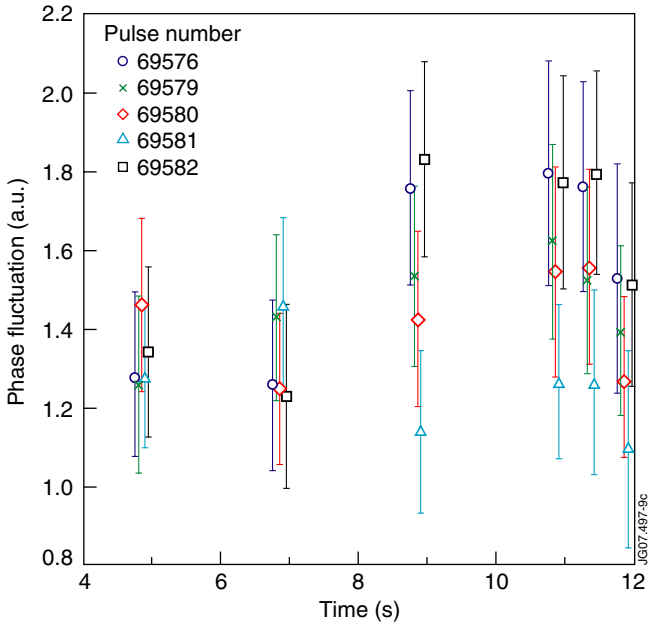

Figure 11. Fluctuation level measured by O-mode reflectometry just inside the LCFS (cut-off density $= 1.1 \times 10^{19}\,\mathrm{m}^{-3}$).

to distinguish the private space of the LH launcher. The private space between the limiters is important for the coupling as the density in this region may decrease to values below the cut-off density. This model then allows studying various gas puffing options, e.g. outer mid-plane (as is used for the LH coupling improvement in JET) or top gas injection (the location of which is foreseen to provide the main gas injection in ITER). However, since the model is 2D the gas puff location is always magnetically connected to the LH launcher, and it is impossible to distinguish between connected or not connected cases.

The results of the simulations with different gas puff locations, with and without heating, are shown in figure 12. The figure shows the effect of gas injection at a level of $1 \times 10^{22}\,\mathrm{el\,s}^{-1}$, without any direct SOL heating by LH waves (dashed curves with squares and circles) and with heating 50 kW (full curves with squares and circles). Gas injection at the outer mid-plane (squares) is clearly more favourable for increasing the density at the outer mid-plane than gas injection from the top (circles). However, the density at the wall (LH launcher position) increases to $1 \times 10^{18}\,\mathrm{m}^{-3}$ with both gas puffing locations when considering SOL heating, although the outer mid-plane gas puffing is the more favourable. This modelling indicates that gas puffing from the top of the torus could also be suitable for improving the LH coupling in ITER. Further experiments to verify this have therefore been proposed in JET.

6. Summary and conclusions

Good coupling of LHCD power in H-mode plasmas with high frequency type I ELMs, at high triangularity and ITER-relevant plasma–launcher distance, has been demonstrated in JET. 2.7 MW of LHCD power has been maintained during 8 s with a distance of 14 cm between the LCFS and the launcher. Higher LHCD power has been coupled for shorter periods

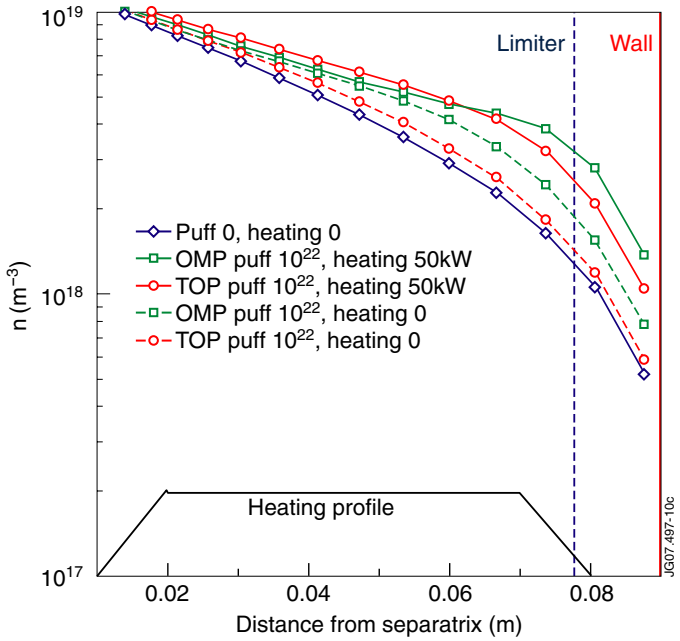

Figure 12. EDGE-2D modelling of the far SOL during gas puffing in JET for the configuration of pulse #66972: electron density profile at the outer mid-plane with gas puffing at 1×10^{22} el s^{-1} from the outer mid-plane (squares) and from the top of the torus (circles). Dashed curves are with zero heating, full curves (squares and circles) are with heating 50 kW. The reference profile without gas puffing and with zero heating is indicated with diamonds.

(3.1 MW/3 s) at 15 cm distance between the LCFS and the launcher. At large LCFS–launcher distance, gas injection in the SOL magnetically connected to the LH launcher is an essential tool for ensuring good coupling. RCP measurements show that the ion saturation current profile flattens in the far SOL, resulting in an increase in electron density in front of the LH launcher.

The modelling effort using the 2D code EDGE-2D confirms the increased density when using both gas puffing and LHCD power. Simulations varying the gas puffing location suggest that the outer mid-plane is obviously the most favourable, but that gas puffing from the top of the torus could also be efficient. However, a 3D analysis would be needed to fully model the SOL during gas puffing. The possibility to use gas injection from the top of the torus to improve LH coupling will be investigated in future experiments in JET.

The effect of gas injection, as needed for LH coupling, on the plasma performance was investigated during the LH coupling experiments. However, the experiments were performed in scenarios with modest normalized H-mode confinement, H98(y,2), that are not representative of the highest performance scenarios in JET. From the available data, no difference between gas injection near the LH launcher or from the divertor can be found. In the scenarios studied, H98(y,2) decreases as the density normalized to the Greenwald density limit increases, whether gas is puffed near the launcher or far away from it. A more systematic study in higher confinement regimes is planned in order to verify that the gas injection near the LH launcher (outer mid-plane) does not have a greater influence on confinement degradation than gas injection from other locations.

The effect on the LH CD efficiency during near gas puffing has also been investigated. The results obtained seem to indicate a modest decrease in LH driven current (by $\sim$15%) at

large LCFS–launcher distance assisted by near gas injection, compared with the case with small distance between the LCFS and the launcher, where near gas injection is not needed. It should be noted that such a modest decrease in CD efficiency is indeed small in comparison with what would be the loss of coupled LHCD power if not assisted by local gas injection at large distance. In JET experiments, the LHCD power can decrease by typically 75%, if near gas injection is not used in poor LH coupling conditions.

In conclusion, the experiments presented here do not indicate any drastic negative effects either in confinement, or in LH CD efficiency, linked to the near gas injection used for improving the LH coupling at ITER-relevant plasma–launcher distances. This suggests that local gas injection near the LH launcher is a viable method for assuring good coupling conditions in ITER plasmas.

Acknowledgments

The authors acknowledge the support of the UKAEA JET Operator of the JET EFDA Facility. The support of the UKAEA Heating and Fuelling Department, and in particular of the LHCD Team, is gratefully acknowledged. This work, supported by the European Communities under the contract of Association between EURATOM and CEA, was carried out within the framework of the European Fusion Development Agreement. The views and opinions expressed herein do not necessarily reflect those of the European Commission. One of the authors (V Petrzilka) was supported in part by the Czech Science Foundation Project GACR 202/07/0044 and by MSMT CR Grant No LA08048.

References

[1] Bonoli P T *et al* 2003 *Proc. 15th Topical Conf. on Radio Frequency Power in Plasmas (Moran, WY) AIP Conf. Proc.* **694** 24–37
[2] Challis C 2004 *Plasma Phys. Control. Fusion* **46** B23–40
[3] Mailloux J *et al* 2002 *Phys. Plasmas* **9** 2156
[4] Leuterer F *et al* 1991 *Plasma Phys. Control. Fusion* **33** 169
[5] Lennholm M *et al* 1995 *Proc. 16th Symp. on Fusion Engineering (Urbana–Champaign, IL)* vol 1 p 754
[6] Schild Ph *et al* 1997 *Proc. 17th Symp. on Fusion Engineering (San Diego, CA)* vol 1 p 421
[7] Pericoli Ridolfini V *et al* 2004 *Plasma Phys. Control. Fusion* **46** 349
[8] Ekedahl A *et al* 2005 *Nucl. Fusion* **45** 351
[9] Rantamäki K *et al* 2007 *Proc. 17th Topical Conf. on Radio Frequency Power in Plasmas (Clearwater, FL) AIP Conf. Proc.* **933** 261–4
[10] Mayoral M-L *et al* 2007 *Proc. 17th Topical Conf. on Radio Frequency Power in Plasmas (Clearwater, FL) AIP Conf. Proc.* **933** 55–58
[11] Erents S K *et al* 2000 *Plasma Phys. Control. Fusion* **42** 905
[12] Joffrin E *et al* 2005 *Nucl. Fusion* **45** 626
[13] Stix T H 1962 *The Theory of Plasma Waves* (New York: McGraw-Hill)
[14] Golant V E 1972 *Sov. Phys.—Tech. Phys.* **16** 1980
[15] Ikeda Y *et al* 1994 *Nucl. Fusion* **34** 871
[16] Ekedahl A *et al* 2001 *Proc. 14th Topical Conf. on Radio Frequency Power in Plasmas (Oxnard, CA, USA, 2001)* (New York: Melville) *AIP Conf. Proc.* **595** 249–52
[17] Saibene G *et al* 1999 *Nucl. Fusion* **39** 1133
[18] ITER Physics Basis Editors 1999 *Nucl. Fusion* **39** 2175
[19] Greenwald M *et al* 1988 *Nucl. Fusion* **28** 2199
[20] Castaldo C *et al* 2002 *Phys. Plasmas* **9** 3205
[21] Cesario R *et al* 2007 *Proc. 34th EPS Conf. on Plasma Physics (Warsaw)*
[22] Imbeaux F and Peysson Y 2005 *Plasma Phys. Control. Fusion* **47** 2041

[23] Basiuk V *et al* 2003 *Nucl. Fusion* **43** 822
[24] Buttery R *et al* 2003 *Nucl. Fusion* **43** 69
[25] Cesario R *et al* 2006 *Nucl. Fusion* **46** 462
[26] de Andrade M C R *et al* 1994 *Plasma Phys. Control. Fusion* **36** 1171
[27] Goniche M *et al* 1997 JET-R(97)14 *JET Internal Report* JET Joint Undertaking, Abingdon, Oxon OX14 3EA, UK
[28] Simonini R, Corrigan G, Radford G, Spence J and Taroni A 1994 *Contrib. Plasma Phys.* **34** 368–73
[29] Petrzilka V *et al* 2006 SOL Ionization by the lower hybrid wave during gas puffing *Proc. 33rd EPS Conf. on Plasma Physics (Rome, Italy)* paper P-1.06
[30] Petrzilka V *et al* 2007 Near LH grill density variations as a function of gas puff and LH power *Proc. 34th EPS Conf. on Plasma Physics (Warsaw, Poland)* paper P4.100